

The EUMETSAT Satellite Application Facility on Land Surface Analysis (LSA SAF)

Validation Report Fire Detection and Monitoring (FD&M)

PRODUCT: LSA-501

The EUMETSAT
Network of
Satellite Application
Facilities



Reference Number:
Issue/Revision Index:
Last Change:

SAF/LAND/IPMA/VR_FD&M/V
Issue V
01/08/2016

	VR-FD&M	Doc: SAF/LAND/IPMA/VR_FD&M/V Issue: Version V Date: 01/08/2016
---	--------------------	--

DOCUMENT SIGNATURE TABLE

	Name	Date	Signature
Prepared by :	Carlos C. DaCamara, Teresa J. Calado, Sofia L. Ermida, Teresa L. Rosa and Sílvia A. Nunes		
Approved by :	Land SAF Project Manager (IPMA)		

DOCUMENTATION CHANGE RECORD

Issue / Revision	Date	Description:
Version I/2010	08/03/2010	Version to be presented to ORR
Version II/2011	23/05/2011	Changes following the ORR meeting of April 2010: (1) The validation report was updated with the aim of demonstrating that the accuracy requirements are fulfilled; (2) Results related to the comparison with the FRP pixel (LSA-31) are not included.
Version III/2013	12/10/2013	Version presented to the ORR.
Version IV/2014	11/11/2015	Version addressing action issued from ORR Section 1 – this section is now more concise Section 2 – requirements table is included Section 3 from version III was removed Section 4 from version III was entirely rewritten to address the issues raised by the reviewers and is now section 3 A new section 4 with conclusions is now included
Version V/2016	01/08/2016	Documentation change record for version IV was included This sentence “). Similar results (not shown) were also obtained for higher latitudes of Europe and for Ukraine.” was included in section 2, page 15

DISTRIBUTION LIST

Internal Consortium Distribution		
Organisation	Name	No. Copies
IPMA	Isabel Trigo	
IPMA	Sandra Coelho e Freitas	
IPMA	Carla Barroso	
IPMA	Isabel Monteiro	
IPMA	João Paulo Martins	
IPMA	Pedro Diegues	
IPMA	Ana Veloso	
IPMA	Pedro Ferreira	
IDL	Carlos da Camara	
IDL	Teresa Calado	
KIT	Folke-S. Olesen	
KIT	Frank Goettsche	
MF	Jean-Louis Roujean	
MF	Gregoire Jacob	
MF	Dominique Carrer	
RMI	Françoise Meulenberghs	
RMI	Arboleda Alirio	
RMI	Nicolas Ghilain	
UV	Joaquin Melia	
UV	F. Javier García Haro	
UV/EOLAB	Fernando Camacho	
UV	Aleixander Verger	

External Distribution		
Organisation	Name	No. Copies
EUMETSAT	Frédéric Gasiglia	
EUMETSAT	Dominique Faucher	
EUMETSAT	Lorenzo Sarlo	
EUMETSAT	Lothar Schueller	
EDISOFT	Teresa Cardoso	
EDISOFT	Joana Rosa	
EDISOFT	Joaquim Araújo	
SKYSOFT	Mauro Lima	

Table of Contents

DOCUMENT SIGNATURE TABLE2

DOCUMENTATION CHANGE RECORD.....2

1. Introduction6

2. Product characteristics6

3. Product validation.....17

 3.1. Rationale.....17

 3.2. Method17

 3.3. Results18

4. Conclusion20

5. References21

List of Tables

Table 1. Requirements of the Fire Detection and Monitoring Product – 2 (FD&M-2).	7
Table 2. Results of validation exercise: areas and periods under analysis, number of identified events, by SEVIRI alone, by both SEVIRI and MODIS, and by MODIS alone, respectively, probability of detection and false alarm rate.	19

List of Figures

Figure 1. Schematic overview of the processing stages of FiDAlgo.	8
Figure 2. Fire pixels over the African continent during January 2015. The colour of each fire pixel is according to the number of active fires identified. The black box delimits an area where the spatial distribution of fire activity and its daily cycle are analysed.	8
Figure 3. As in Figure 2 but for fire pixels over the entire MSG disk during July 2015.	9
Figure 4. As in Figure 3 but during August 2015.	10
Figure 5. As in Figure 3 but during September 2015.	10
Figure 6. Fire activity during January 2015 over the selected region in northern Africa; land cover based on GLC2000 (upper panel), spatial distribution of fire pixels and active fires (middle panel) and daily cycle of fire activity (lower panel). The selected region is defined by the black box in Figure 2 and is delimited by lines 1500 and 1700 and by columns 2800 and 3000 of the MSG disk.	11
Figure 7. As in Figure 6 but for fire activity during July 2015 over the selected region in Southern Africa. The selected region is defined by the black box in Figure 3 and is delimited by lines 2100 and 2300 and by columns 2450 and 2650 of the MSG disk.	12
Figure 8. As in Figure 6 but for fire activity during August 2015 over the selected region in the Iberian Peninsula. The selected region is defined by the black box in Figure 4 and is delimited by lines 450 and 650 and by columns 1600 and 1800 of the MSG disk.	13
Figure 9. As in Figure 6 but for fire activity during September 2015 over the selected region in Brazil. The selected region is defined by the black box in Figure 5 and is delimited by lines 2200 and 2400 and by columns 300 and 600 of the MSG disk.	14
Figure 10. Weekly cycles of fire activity in the African continent and its relation to the geographical distribution of religious affiliations as displayed in the bottom left corner (Christian in red, Islamic in green, Animist in grey).	16
Figure 11. The five defined regions for validation	19

	<p style="text-align: center;">VR-FD&M</p>	<p>Doc: SAF/LAND/IPMA/VR_FD&M/V Issue: Version V Date: 01/08/2016</p>
---	--	---

1. Introduction

Geostationary meteorological satellite systems provide much higher frequency of observation of the land surface than sun-synchronous systems but, until recently, their spatial and spectral resolutions were sub-optimal for vegetation fire monitoring. Nevertheless, various authors demonstrated the capability of earlier geostationary satellites to detect active fires (Prins & Menzel, 1992, 1994; Prins & Schmetz, 2000) and to estimate burned areas (Boschetti et al., 2003).

New possibilities were opened up with the launch in 2002, by the European Space Agency (ESA) in cooperation with the European Organisation for the Exploitation of Meteorological Satellites (EUMETSAT), of Meteosat-8, the first satellite of the Meteosat Second Generation (MSG). Temporal, spatial and spectral characteristics of the MSG series were substantially improved (Schmetz et al., 2002), rendering its satellites very adequate for Earth surface observation, and namely for fire monitoring (Cihlar et al., 1999; Pereira & Govaerts, 2001). The potential of MSG was promptly explored, namely by expanding the scope of previous fire applications of geostationary systems with the goal of quantifying fire intensity and biomass consumption (Roberts et al., 2005; Roberts & Wooster, 2008; Roberts et al., 2015; Wooster et al., 2015). Information about fire activity has also been used to calibrate indices of fire danger and generate maps with classes of fire danger (Amraoui *et al.*, 2013; DaCamara *et al.*, 2014; Amraoui *et al.*, 2015).

Developed within the framework of the LSA SAF, FiDAIgo is a contextual algorithm for detecting active fires, every 15-min using information provided by MSG at the maximum temporal resolution (Amraoui *et al.*, 2010). The algorithm was on the basis of the LSA-501 product, referred to as the Fire Detection and Monitoring (FD&M) product. Product LSA-501 was superseded by product LSA-512, referred to as product Fire Detection and Monitoring 2; information about the product is provided in Table 1.

This document presents the characteristics of FD&M and reports on results obtained from a comprehensive validation exercise of the product. For this purpose, the product will be tested over northern Africa, southern Africa, Europe and South America during periods of enhanced fire activity, from 2013 to 2015. Maps of active fires produced every 15-min will then be compared against independent data, namely those from the MODIS Fire Team product (Justice *et al.*, 2002).

This document is organized as follows; first a description is provided of the FD&M product (LSA 501) focusing on spatial and temporal characteristics of the FD&M. Then the validation procedure is thoroughly described and results obtained are presented and discussed. The document ends with a section presenting the concluding remarks.

2. Product characteristics

The FD&M product is based on the so-called FiDAIgo algorithm which takes advantage of the temporal resolution of SEVIRI (one image every 15 min), and relies on information from SEVIRI channels (namely 0.6, 0.8, 3.9, 10.8 and 12.0 μm) together with information on illumination angles. The method is based on heritage from contextual algorithms designed for polar, sun-synchronous instruments, namely NOAA/AVHRR and MODIS/TERRA-AQUA (Amraoui et al., 2010).

	<p style="text-align: center;">VR-FD&M</p>	<p>Doc: SAF/LAND/IPMA/VR_FD&M/V Issue: Version V Date: 01/08/2016</p>
---	--	---

Table 1. Requirements of the Fire Detection and Monitoring Product – 2 (FD&M-2).

LSA-512		Fire Detection and Monitoring – 2		FD&M
Type	Product			
Applications and users	Research or Environmental monitoring			
Characteristics and Methods	Contextual analysis of IR3.9 and IR10.8 and dynamic thresholds taking advantage of SEVIRI temporal frequency			
Comments	This product will supersede LSA-501.			
Generation frequency	15-min			
Input satellite data	MSG: SEVIRI			
Dissemination				
Format		Means		Type
HDF5		EUMETCast, HTTP		NRT, Offline
Accuracy				
Threshold		Target		Optimal
A successful detection of a significant fraction of active fires such that the spatial and temporal distribution is adequately reproduced.		POD=25% FAR=30% Computed against MODIS fires with FRP> 50 MW on a 3x3 MSG pixel grid		POD=50% FAR=20% Computed against MODIS fires with FRP> 50 MW on a 3x3 MSG pixel grid
Verification method		MODIS		
Coverage, resolution and timeliness				
Spatial coverage		Spatial resolution		Vertical resolution
MSG disk		SEVIRI pixel Resolution		Timeliness 3 h

A potential fire pixel is compared with the neighbouring ones and the decision is made based on relative thresholds as derived from the pixels in the neighbourhood. As schematically shown in Fig. 1, the method consists of the following four main steps; 1) Pre-processing, 2) Selection of potential fire pixels, 3) Detection of contaminated pixels and 4) Confirmation of active fire pixels. Details about the procedure may be found in the ATBD of the FD&M product (document SAF/LAND/IM/ATBD_FD&M/03).

The procedure allows identifying both active fires (i.e. occurrences in a given pixel of a given image) and fire pixels (i.e. pixels where at least one active fire was detected, throughout the study period). Figure 2 presents the spatial distribution of identified active fires and fire pixels over the African

continent during January 2015. Most burning activity may be found in the region of Sudan, especially in southern Chad, in the Central African Republic, southern Sudan and in various regions of West Africa; lower fire activity may be also noticed in a vast area along the west and south coast of southern Africa and in the north and south tips of Madagascar.

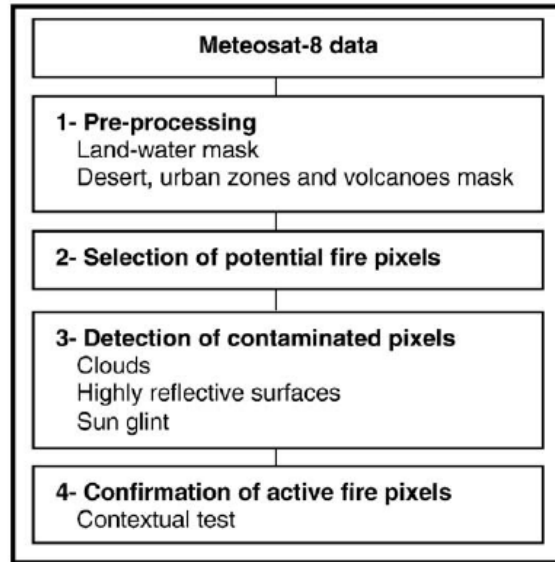


Figure 1. Schematic overview of the processing stages of FiDALgo.

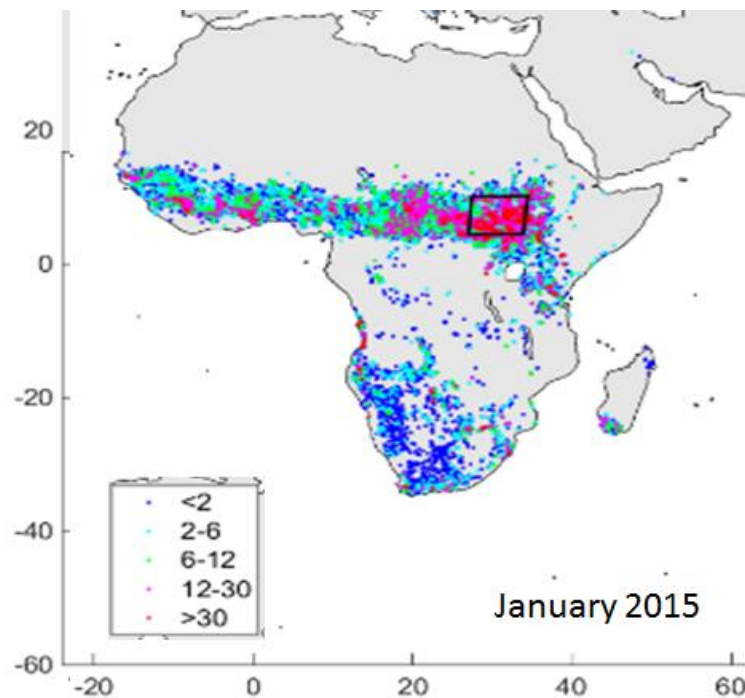


Figure 2. Fire pixels over the African continent during January 2015. The colour of each fire pixel is according to the number of active fires identified. The black box delimits an area where the spatial distribution of fire activity and its daily cycle are analysed.

Figures 3 to 5 present the spatial distribution of identified active fires and fire pixels over the entire MSG disk during July, August and September 2015, respectively. Regions of high burning activity may be observed in southern Africa, namely in northern Angola, the southern Democratic Republic of Congo and western Zambia as well as in South America, in Brazil, Bolivia and Colombia. A belt of burning activity, albeit less intense, may also be observed in the tropical savannas of northern Africa. Fire activity is also present in the Mediterranean coast of North Africa (Morocco, Algeria and Tunisia) and in southern Europe, especially in the Iberian Peninsula, Italy, the Balkans, Greece and Turkey, around the Black Sea, Moldavia, Ukraine and South Russia.

Figures 6 to 9 present a more detailed view of the spatial and temporal characteristics of fire activity in northern Africa, southern Africa, the Iberian Peninsula and Brazil, respectively. The selected region located in northern Africa (Figure 6) mostly consists of “shrub cover, closed open, deciduous” (43%), “Tree cover, broadleaved, deciduous, open” (17%) and by “Mosaic: cropland/shrub or grass cover” (17%). High burning activity (red and orange dots) mainly occurs over shrub. The daily cycle of active fires presents a slightly asymmetric distribution, with a well-defined peak located around 11:30 UTC (~13:30 solar time), with a steeper increase before the maximum and a slower decrease during the afternoon that presents a secondary peak around 15:00 UTC (~17:00 solar time); there is virtually no fire activity between 22:00 and 07:00 UTC (~00:00 and ~09:00 solar time).

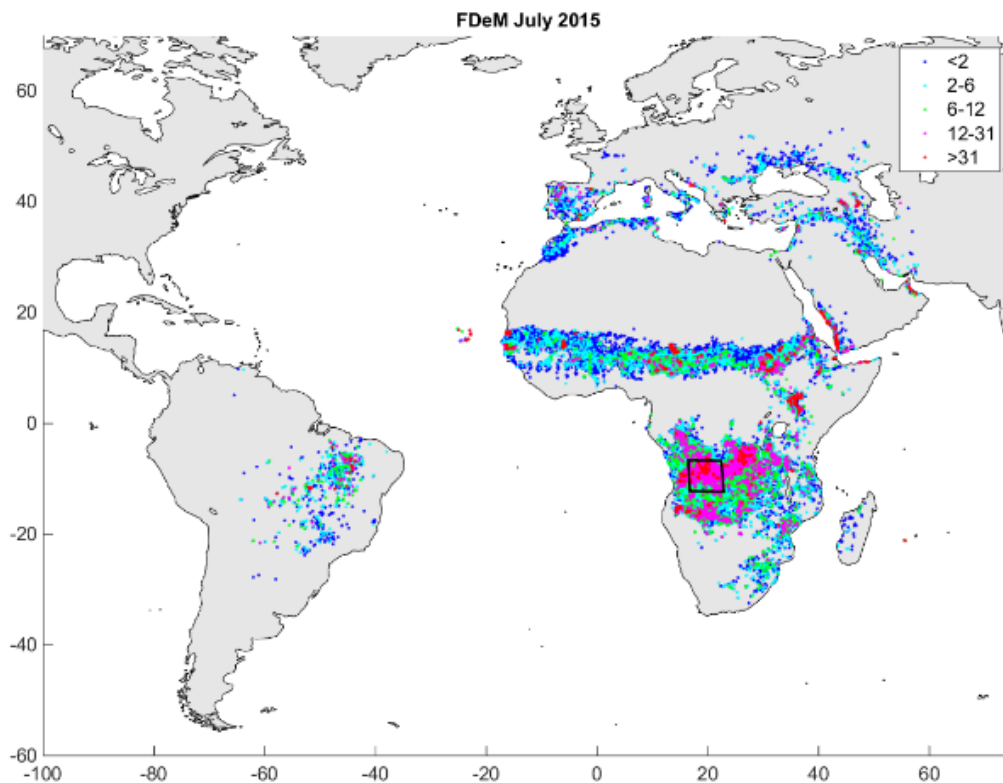


Figure 3. As in Figure 2 but for fire pixels over the entire MSG disk during July 2015.

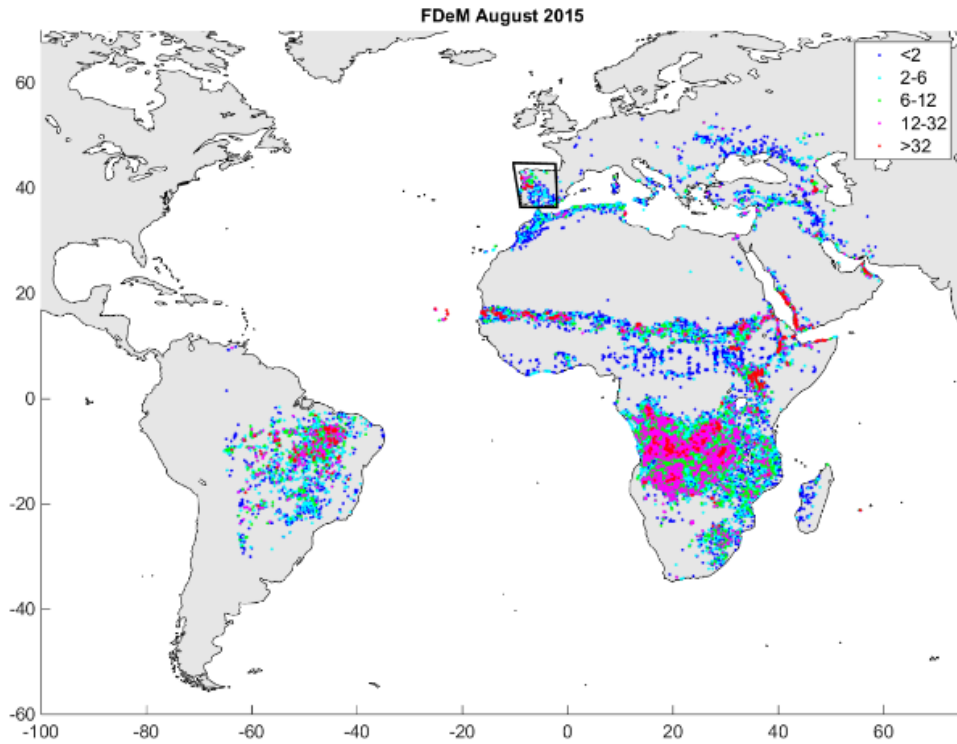


Figure 4. As in Figure 3 but during August 2015.

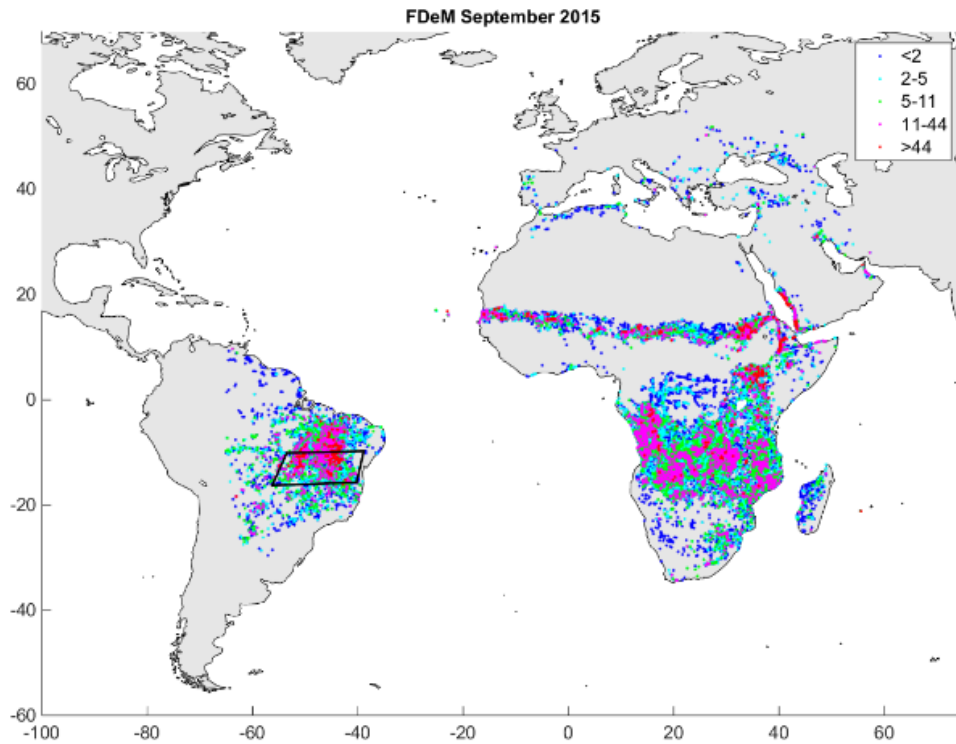
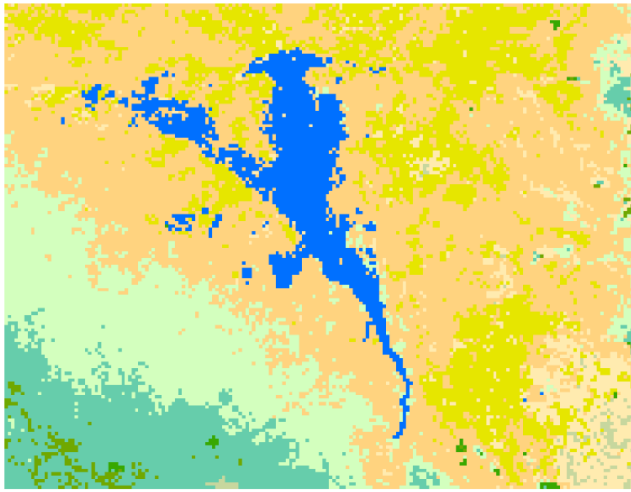
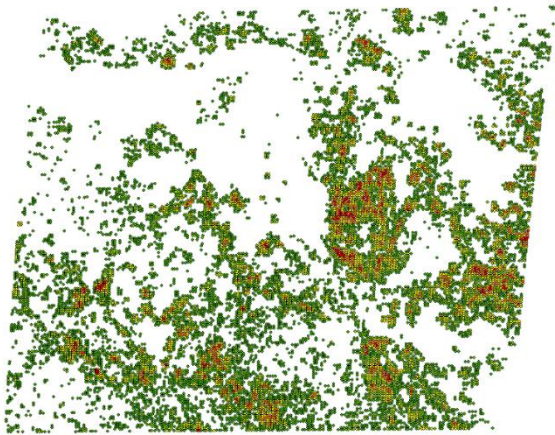


Figure 5. As in Figure 3 but during September 2015.



- Tree cover, broadleaved, evergreen
- Tree cover, broadleaved, deciduous, closed
- Tree cover, broadleaved, deciduous, open
- Tree cover, needle-leaved, evergreen
- Tree cover, needle-leaved, deciduous
- Tree cover, mixed leaf type
- Tree cover, regularly flooded, fresh water
- Tree cover, regularly flooded, saline water
- Mosaic: tree cover/other natural vegetation
- Tree cover, burnt
- Shrub cover, closed-open, evergreen
- Shrub cover, closed-open, deciduous
- Herbaceous cover, closed-open
- Sparse herbaceous or sparse shrub cover
- Regularly flooded shrub and/or herbaceous cover
- Cultivated and managed areas
- Mosaic: cropland/tree cover/other natural vegetation
- Mosaic: cropland/ shrub or grass cover
- Bare areas
- Water bodies
- Snow and Ice
- Artificial surfaces and associated areas



- ◆ <2
- ◆ 2-10
- ◆ 10-22
- ◆ 22-44
- ◆ 44-94

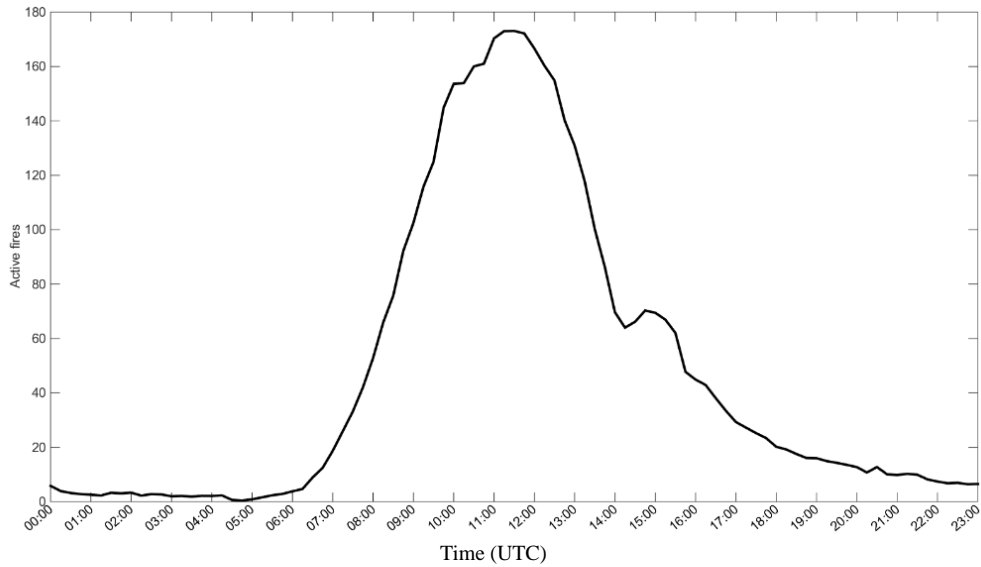


Figure 6. Fire activity during January 2015 over the selected region in northern Africa; land cover based on GLC2000 (upper panel), spatial distribution of fire pixels and active fires (middle panel) and daily cycle of fire activity (lower panel). The selected region is defined by the black box in Figure 2 and is delimited by lines 1500 and 1700 and by columns 2800 and 3000 of the MSG disk.

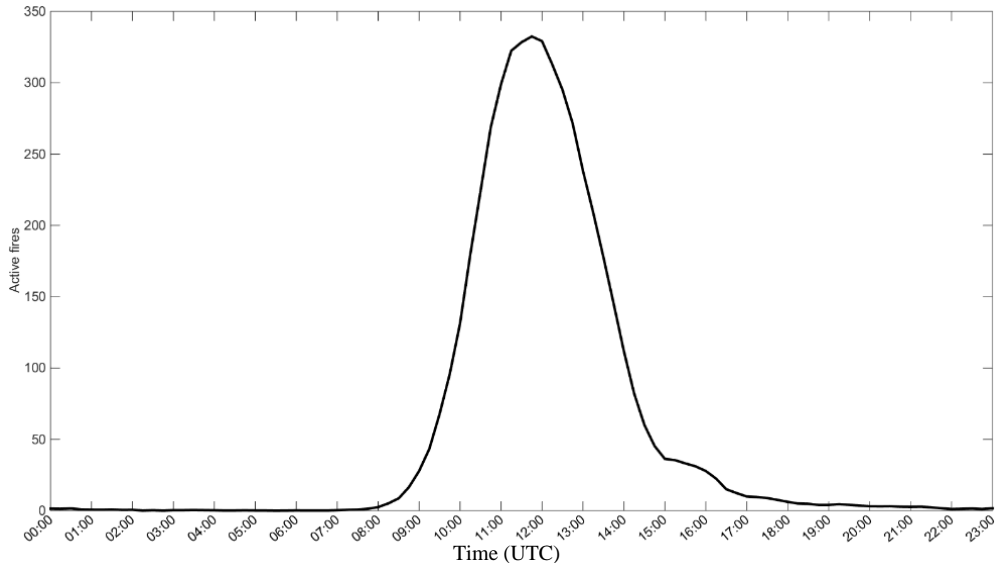
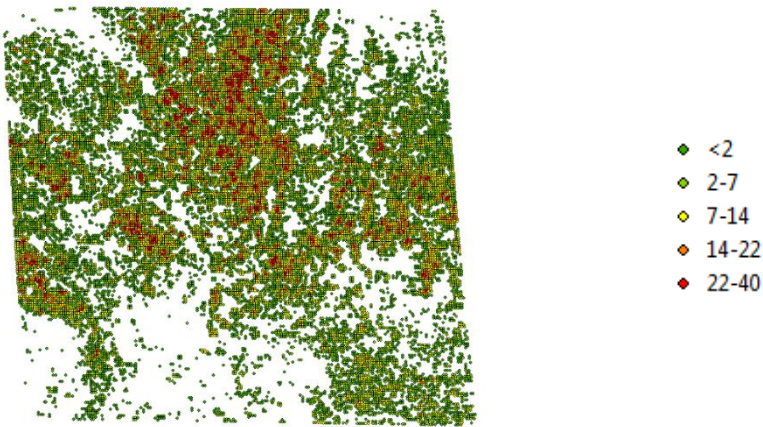
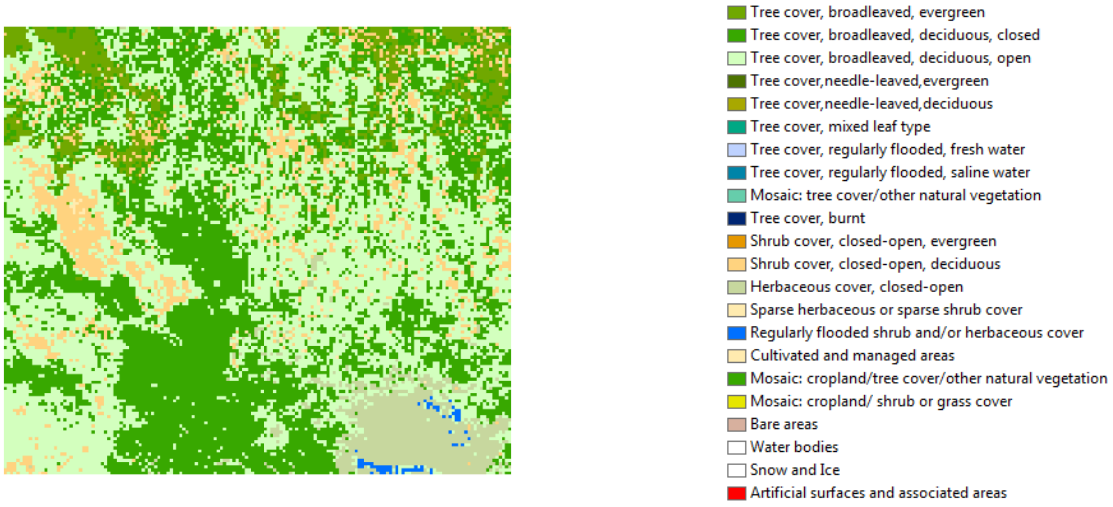


Figure 7. As in Figure 6 but for fire activity during July 2015 over the selected region in Southern Africa. The selected region is defined by the black box in Figure 3 and is delimited by lines 2100 and 2300 and by columns 2450 and 2650 of the MSG disk.

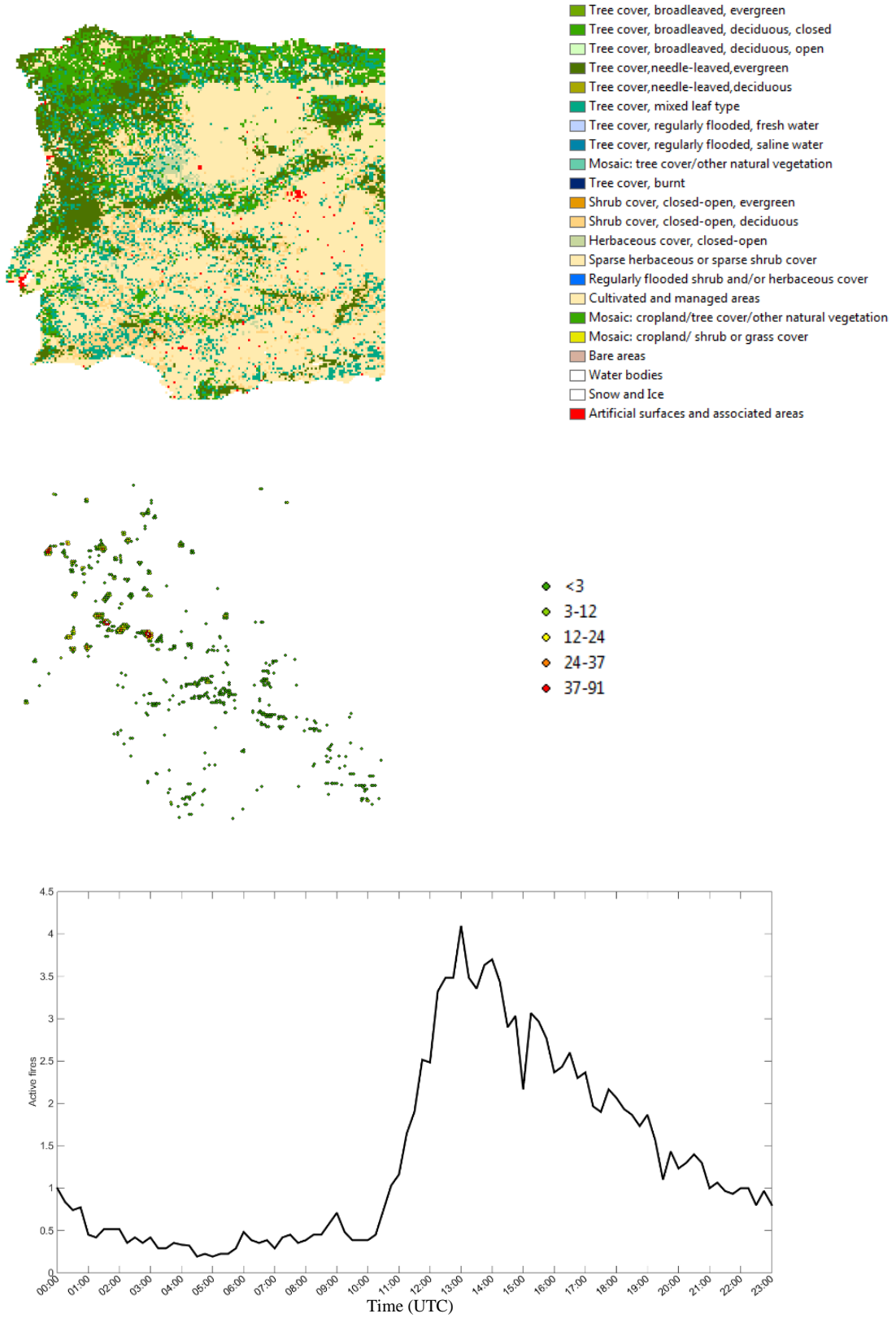


Figure 8. As in Figure 6 but for fire activity during August 2015 over the selected region in the Iberian Peninsula. The selected region is defined by the black box in Figure 4 and is delimited by lines 450 and 650 and by columns 1600 and 1800 of the MSG disk.

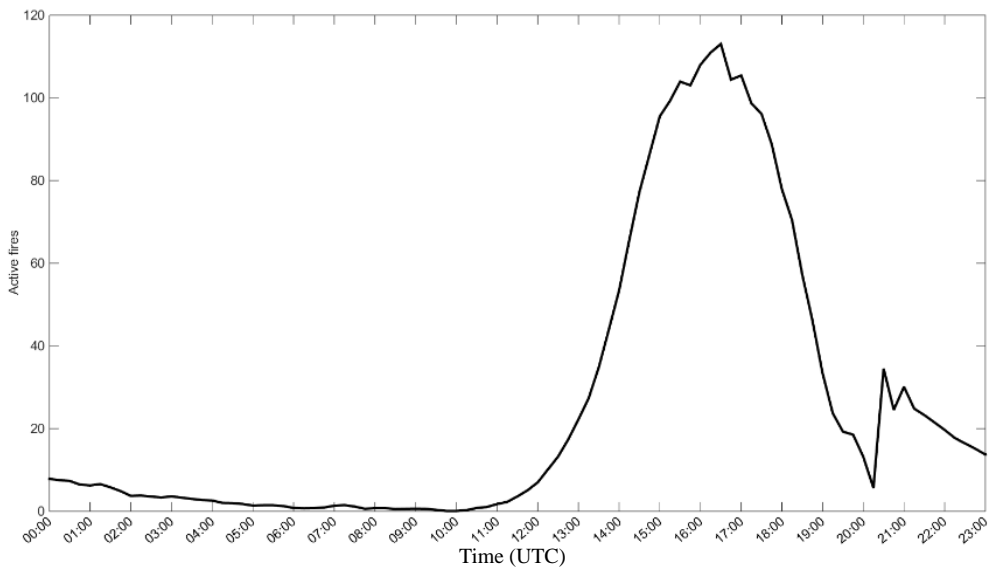
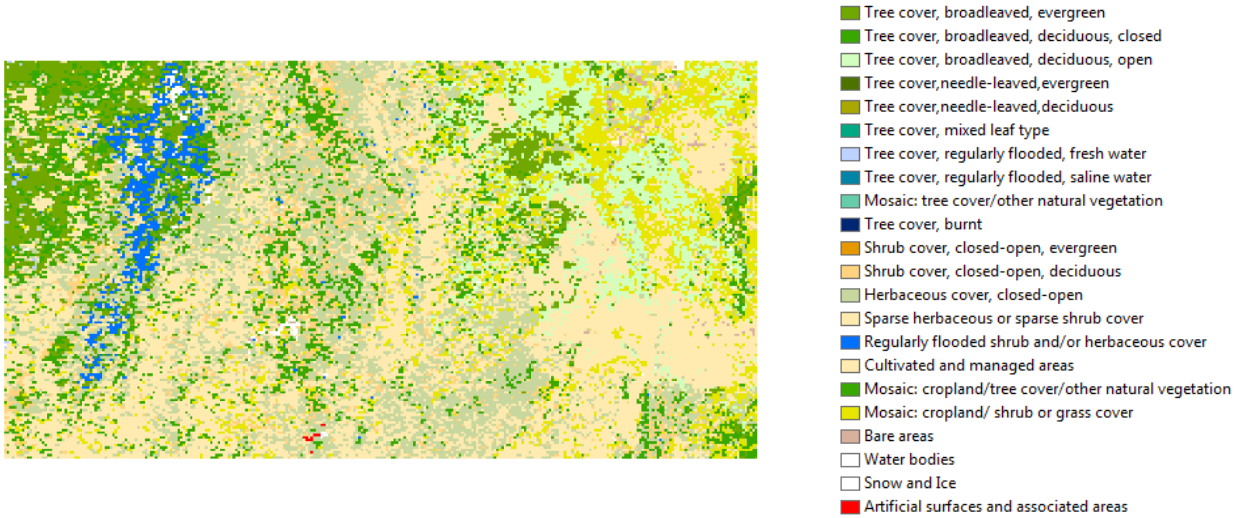


Figure 9. As in Figure 6 but for fire activity during September 2015 over the selected region in Brazil. The selected region is defined by the black box in Figure 5 and is delimited by lines 2200 and 2400 and by columns 300 and 600 of the MSG disk.

	<p>VR-FD&M</p>	<p>Doc: SAF/LAND/IPMA/VR_FD&M/V Issue: Version V Date: 01/08/2016</p>
---	--------------------	---

The selected region over southern Africa (Figure 7) mainly consists of “tree cover, broadleaved, deciduous, open” (41%) followed by “tree cover, broadleaved, deciduous, closed” (39%). Burning activity tends to occur over the first class mentioned. The daily cycle is more symmetrical than in the case of northern Africa and the peak is around 12:00 UTC (~13:00 solar time); a trace of a secondary peak about 16:00 UTC (~17:00 solar time) is also observed.

The selected region over the Iberian Peninsula (Figure 8) is mostly covered by “cultivated and managed areas” (48%), followed by “tree cover, mixed leaf type” (13%), “tree cover, needle-leaved, evergreen” (13%), “tree cover broadleaved, deciduous, closed” (11%) and “shrub cover, closed-open, deciduous” (11%). Highest fire activity (red and orange dots) mainly occurs in “tree cover, needle-leaved, evergreen”. The daily cycle is highly asymmetric with a sharp increase from 10:00 to 13:00 UTC (~10:00 to ~13:00 solar time) when there is a peak of fire activity, followed by a slow decrease until 02:00 UTC (~02:00 solar time). There is almost no activity between 02:00 and 10:00 UTC (~02:00 and ~10:00 solar time).

Finally, the selected region over Brazil (Figure 9) is mostly covered by “cultivated and managed areas” (32%) followed by “herbaceous cover, closed-open” (21%) and by “mosaic: croplands/shrub or grass cover” (11%). sparse vegetation. There is no preferred vegetation cover for highest burning activity. The daily cycle of fire activity is again more symmetrical, with a sharp peak centred at 16:30 UTM (~13:30 solar time) and a quite large secondary peak between 21:00 and 22:00 UTC (~18:00 and ~19:00 solar time). Similar results (not shown) were also obtained for higher latitudes of Europe and for Ukraine.

The calibration/validation of the FiDAlgo algorithm has also unveiled an interesting weekly cycle of fire activity in the African continent related to religious affiliations; as shown in Figure 10, regions where the Christian affiliation is dominant present lower fire activity on Sundays as opposed to lower fire activity on Fridays that is observed in regions where the Islamic affiliation predominates (DaCamara, 2011). This weekly cycle has been recently thoroughly investigated by Pereira et al. (2015) based on 9 years of MODIS data.

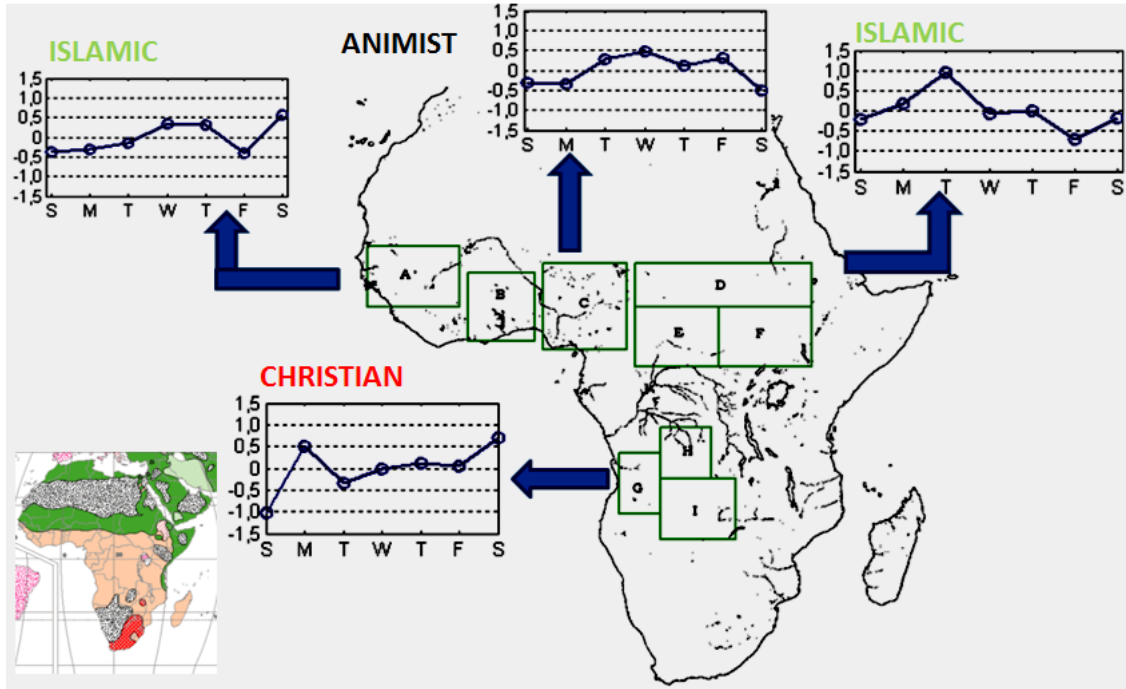


Figure 10. Weekly cycles of fire activity in the African continent and its relation to the geographical distribution of religious affiliations as displayed in the bottom left corner (Christian in red, Islamic in green, Animist in grey).

	VR-FD&M	Doc: SAF/LAND/IPMA/VR_FD&M/V Issue: Version V Date: 01/08/2016
---	--------------------	--

3. Product validation

3.1. Rationale

In the case of detection and monitoring of active vegetation fires, any validation procedure involves checking at least the following two key aspects of the developed detection algorithm; i) whether it is sensitive, minimizing *omission errors* (i.e. missed hits), and ii) whether it is selective, minimizing *commission errors* (or false alarms).

The FD&M product is based on information from SEVIRI on-board Meteosat which is provided at a very high temporal resolution (i.e. images with a 15-minute repeat cycle). However the spatial resolution is rather low, corresponding to $3 \times 3 \text{ km}^2$ at the sub-satellite point (SSP) and decreasing with increasing distance from SSP.

The MODIS active fire data consist of hot spots as detected by the MODIS radiometer on-board the polar-orbiting Terra and Aqua platforms. The MODIS fire detection algorithm is based on a contextual algorithm developed by Giglio *et al.* (2003). Information is obtained from thermal channels at coarse spatial resolution (i.e. with a pixel size of the order of $1 \times 1 \text{ km}^2$) and with a low temporal resolution consisting of four observations per day (Justice *et al.*, 2002) and corresponding to the maximum temporal resolution of the above mentioned radiometer. The MODIS active fire data is part of the MODIS Fire Products that include an identification of the occurrence of thermal anomalies, as well as estimates of the total emitted power from the fire and of the burned area.

When validating FD&M against the MODIS fire product, one has to keep in mind that when comparing data from geostationary sensors, such as SEVIRI, with those from polar-orbit sensors, such as MODIS, the different spatial and temporal resolutions of the two instruments have to be accounted for. Moreover, when the comparison involves data from polar sensors with finer spatial resolution, then the procedure is especially complex due to errors caused by data misregistration (Calle *et al.*, 2008).

3.2. Method

Validation is performed using as reference MODIS data, for both TERRA and AQUA sensors. Taking into account the different spatial resolution of SEVIRI ($3 \times 3 \text{ km}^2$) and TERRA/AQUA ($1 \times 1 \text{ km}^2$) sensors, it was necessary to degrade MODIS data. For that purpose, and for each MSG pixel, the number of MODIS pixels with Viewing Zenith Angle (VZA) lower than 40° , flagged as water, cloud, no fire and fire were counted.

As specified in the LSA SAF Product Requirements Document (document SAF/LAND/PRD/2.8), in order to mitigate errors of georeferencing the comparison is performed on a 3×3 SEVIRI pixel grid (Table 1). On the other hand, in order to insure an appropriate temporal agreement, considered FD&M fires are those that take place in MSG slots immediately before and after each MODIS observation time (e.g. if AQUA observes an active fire at 10:50 UTC, then both 10:45 UTC and 11:00 UTC MSG slots are considered for comparison).

An active fire detection by MSG on a 3×3 SEVIRI pixel grid is considered as eligible and therefore counted as one event when there is at least a fire pixel detected by MSG immediately before or after the MODIS observation time; in turn, an active fire detection by MODIS is considered as eligible and therefore counted as one event if the accumulated power of all detections in the 3×3 SEVIRI pixel exceeds 50 MW.

	VR-FD&M	Doc: SAF/LAND/IPMA/VR_FD&M/V Issue: Version V Date: 01/08/2016
---	---------	--

Evaluation of both FD&M and MODIS products is performed by means statistical measures of accuracy based on contingency tables, namely Probability of Detection (POD) and False Alarm Ratio (FAR). POD is defined as the ratio between the number of events detected by both SEVIRI and MODIS on the 3x3 SEVIRI pixel grid and the total number of events detected by MODIS detections. FAR is computed by dividing the number of events detected by SEVIRI and not detected by MODIS on the 3x3 SEVIRI pixel grid by the total number of events detected by SEVIRI detections.

3.3. Results

The validation exercise was performed over the following areas and periods of time (Figure 10):

1. Northern Africa, a rectangular window defined between lines 700 and 1850 and between columns 1240 and 3450, covering the complete 15-minute cycle of January 2013;
2. Southern Africa, a rectangular window defined between lines 1850 and 3040 and between columns 2140 and 3350, covering the complete 15-minute cycle of June and August 2014;
3. Europe, a rectangular window defined between lines 50 and 700 and between columns 1550 and 2374, covering the complete 15-minute cycle of July 2015;
4. Ukraine, a rectangular window defined between lines 50 and 700 and between columns 2375 and 3250, covering the complete 15-minute cycle of July 2015;
5. South America, a rectangular window defined between lines 1460 and 2970 and columns 40 and 740, covering the complete 15-minute cycle of September 2014.

Choice of areas and periods was motivated by the availability of data and by the number of recorded fire occurrences.

The validation exercise consisted in performing a systematic comparison of the FD&M product against a similar product provided by the MODIS Fire Team (Justice *et al.*, 2002). As specified in the LSA SAF Product Requirements Document (document SAF/LAND/PRD/2.8), the threshold consists in successfully detecting a significant fraction of active fires such that the spatial and temporal distribution is adequately reproduced.

As shown in Table 1 and as specified in the LSA SAF Product Requirements Document (document SAF/LAND/PRD/2.8), the target is a POD of 25% and a FAR of 30% computed against MODIS fires with FRP > 50 MW on a 3x3 MSG pixel grid, whereas the optimal is a POD of 50% and a FAR of 20%.

Results obtained from the validation exercise are shown in Table 2. For both the northern and the southern African windows, and for all three periods analysed (January 2013 and June and August 2014) values of FAR (10%, 8% and 10%) are significantly better than the optimal target of FAR=20% (Table 1) whereas the values of POD (21%, 19% and 20%) are slightly below the target of POD=25% (Table 1).

In the case of the European window, the value of POD (16%) is also below the threshold requirement whereas the value of FAR (31%) slightly exceeds the prescribed threshold of 30% (Table 1). It may be nevertheless noted that the number of events is by far lower than in the African continent (especially those detected by FD&M) and this may have a lever effect on FAR towards higher values because the small number of events detected by FD&M appear in the denominator.

Results for the Ukrainian window do not meet the product requirements, both for POD, where the value (3%) is well below the target of 25% and for FAR, where the value (63%) by large exceeds the target of 30%; the poor quality of results for the Ukrainian window is related to the large size of MSG pixels close to the border of the MSG disk and to the large viewing angle by the SEVIRI instrument over this region; these two effects deteriorate the sensitivity of the algorithm to small and medium-sized fires and to increase the noise of the signal that is easily contaminated by sun glint and highly reflective surfaces.

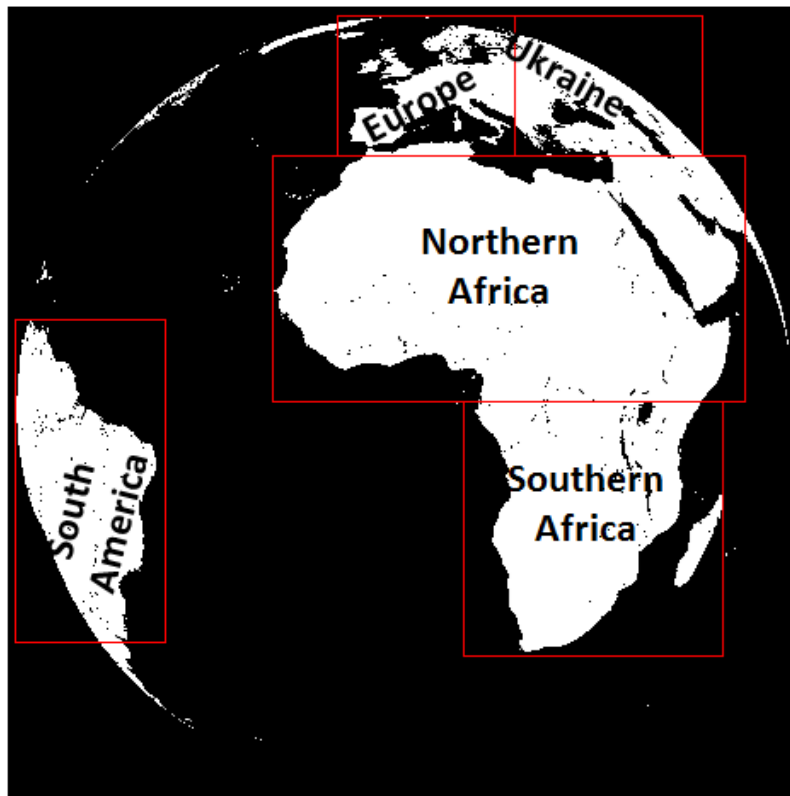


Figure 11. The five defined regions for validation

Table 2. Results of validation exercise: areas and periods under analysis, number of identified events, by SEVIRI alone, by both SEVIRI and MODIS, and by MODIS alone, respectively, probability of detection and false alarm rate.

Location	Time period	FD&M Only [A]	FD&M and MODIS [B]	MODIS Only [C]	POD (%) $100 \times \frac{[B]}{[B] + [C]}$	FAR (%) $100 \times \frac{[A]}{[A] + [B]}$
NorthernAfrica	January 2013	458	4122	15437	21	10
SouthernAfrica	June 2014	278	3110	12936	19	8
	August 2014	545	4732	19346	20	10
Europe	July 2015	16	35	185	16	31
Ukraine	July 2015	79	47	139	3	63
South America	September 2014	136	676	7844	8	17

	VR-FD&M	Doc: SAF/LAND/IPMA/VR_FD&M/V Issue: Version V Date: 01/08/2016
---	--------------------	--

Over the South American window, the value of POD (8%) is well below the prescribed threshold of 25%, but the value of FAR (17%) is below the prescribed optimal threshold of 20%.

Results obtained for the four geographical areas (northern Africa, southern Africa, Europe and South America) consistently indicate that the algorithm currently in operation is conservative in the sense that it provides a very low number of false alarms (that exceeds the optimal target), however at the cost of a relatively low number of correctly identified fire occurrences, slightly below the prescribed target for POD. The same is not true over regions of high viewing angles, located close to the borders of the MSG disk, where results are of poor quality, with a low number of correctly identified fire occurrences and a high number of false alarms.

4. Conclusion

The Fire Detection and Monitoring (FD&M) product is based on a contextual algorithm for detecting active fires, every 15-min (Amraoui *et al.*, 2010). The product allows characterizing the spatial and temporal characteristics of fire activity over a large portion of the continental areas covered by the MSG disk.

In particular, the FD&M product allows identifying regions of high fire activity and relate such activity to characteristics of the vegetation cover. The FD&M product also allows characterizing the daily cycles of fire activity and identifying fire events that persist over time. By combining this information fire regimes may be identified and characterized and then related to meteorological factors and human activity. The latter information is crucial to calibrate indices of meteorological fire danger and to develop statistical models of fire duration for different classes of vegetation cover that allow generating maps of fire danger on an operational basis. Such an approach is on the basis of the Fire Risk Map (FRM) product (LSA-504) where daily maps of fire danger are operationally generated based on integrated use of vegetation cover maps, weather data from meteorological forecasts disseminated by the European Centre for Medium-Range Weather Forecasts (ECMWF) and fire activity as obtained from the FD&M product.

For most of the continental areas inside the MSG disk, the FD&M product is consistent and stable with values of POD of 19-21% in Africa and of 16% in Europe and values of FAR of 8-10% in Africa and 31% in Europe. Over these regions the FD&M product is conservative in the sense that there is a very low number of false alarms (performance of FAR being better than the optimal threshold of 20% in the African continent) and a moderate number of identified number of events that agree with those of MODIS (performance of POD being slightly below the target requirement). Performance of FD&M over Brazil is quite low in terms of number of fire events matching those identified by MODIS (POD of 8%) but, again, the number of false alarms (FAR of 17%) meets the target requirements.

Performance of FD&M is very poor (low values of POD and high values of FAR) for regions located near the edge of the MSG disk where the combination of very large pixels and large viewing angles contribute to lower the sensitivity of the detection algorithm to (medium intensity) fires and where the contamination of the radiative signal by sun glint and reflective surfaces contribute is on the origin of an increased number of false alarms.

Overall, the FD&M product allows characterizing fire activity both in space and time over continental areas and on a routine basis. This is especially relevant for civil protection and forest

	<p style="text-align: center;">VR-FD&M</p>	<p>Doc: SAF/LAND/IPMA/VR_FD&M/V Issue: Version V Date: 01/08/2016</p>
---	--	---

protection authorities to whom the availability of high frequency fire information is an added value. The recognized usefulness of the FRM product (that currently relies on FD&M) by state and private entities in Portugal is worth mentioning in this respect. An increased temporal resolution of vegetation fire data to hourly (or even sub-hourly) intervals is also expected to contribute towards improving models of environmental processes affected by biomass burning.

5. References

- [1] Amraoui, M., C.C. DaCamara, and J.M.C. Pereira (2010). Detection and monitoring of African vegetation fires using MSG-SEVIRI imagery. *Remote Sensing of Environment*, 114 (5), 1038-1052.
- [2] Amraoui M., Liberato M.L.R., Calado T.J., DaCamara C.C., Pinto-Coelho L., Trigo R.M., Gouveia C.M. (2013). Fire activity over Mediterranean Europe based on information from Meteosat-8. *Forest Ecology and Management* 294, 62-75.
- [3] Amraoui M., Pereira M.G., DaCamara C.C., Calado T.J. (2015). Atmospheric conditions associated with extreme fire activity in the Western Mediterranean region. *Science of the Total Environment* 524-525, 32-39. doi: 10.1016/j.scitotenv.2015.04.032.
- [4] Boschetti, L., Brivio, P. A., and Gregoire, J. -M. (2003). The use of Meteosat and GMS imagery to detect burned areas in tropical environments. *Remote Sensing of Environment*, 85, 78–91.
- [5] Calle A., F. Gonzalez-Alonso, and S. Merino de Miguel (2008). Validation of active forest fires detected by MSG-SEVIRI by means of MODIS hot spots and AWiFS images. *International Journal of Remote Sensing*, Vol. 29, 3407-3415.
- [6] Cihlar J., A. Belward and Y. Govaerts (1999). Meteosat Second Generation opportunities for land surface research and applications. EUMETSAT Scientific Publications EUM SP 01.
- [7] DaCamara, C.C. (2011). LSA SAF Week 2011, Session 6: Active fires and burnt areas. EUMETRAIN. Recording and Powerpoint available at http://www.eumetrain.org/resources/vegetation_recovery_2011.html
- [8] DaCamara C.C., Calado T.J., Ermida S.L., Trigo I.F., Amraoui M., Turkman K.F. (2014). Calibration of the Fire Weather Index over Mediterranean Europe based on fire activity retrieved from MSG satellite imagery. *International Journal of Wildland Fire*. doi: 10.1071/WF13157
- [9] Giglio L., J. Descloitres, C.O. Justice and Y.J. Kaufman (2003). An enhanced contextual fire detection algorithm for MODIS. *Remote Sensing of Environment*, Vol. 87, pp. 273-282.
- [10] Justice C.O., L. Giglio, S. Korontzi, J. Owens, J.T. Morisette, D. Roy, J. Descloitres, S. Alleaume, F. Petitcolin and Y. Kaufman (2002). The MODIS fire products. *Remote Sensing of Environment*, Vol. 83, pp. 244-262.
- [11] LSA SAF (2010). Algorithm Theoretical Basis Document for Fire Detection and Monitoring Product (LSA-29), Issue 0.3. Ref. Number SAF/LAND/IM/ATBD_FD&M/03.
- [12] LSA SAF (2015). Product Requirements Document, Version 2.8, Issue 1. Ref. Number SAF/LAND/PRD/2.8
- [13] Pereira J.M.C. and Y. Govaerts (2001). Potential fire applications from MSG/SEVIRI observations. EUMETSAT Programme Development Department, Technical Memorandum No. 7.

	VR-FD&M	Doc: SAF/LAND/IPMA/VR_FD&M/V Issue: Version V Date: 01/08/2016
---	---------	--

- [14] Pereira J.M.C., Oom D., Pereira P., Turkman A.A. and Turkman K.F. (2015) Religious Affiliation Modulates Weekly Cycles of Cropland Burning in Sub-Saharan Africa. *PLoS ONE* 10(9): e0139189.
- [15] Prins, E. M., & Menzel, W. P. (1992). Geostationary satellite detection of biomass burning in Southern America. *International Journal of Remote Sensing*, 13, 2783–2799.
- [16] Prins E.M. and W.P. Menzel (1994). Trends in South American biomass burning detected with the GOES VAS from 1983-1991. *Journal of Geophysical Research*, 99 (D8), pp. 16719-16735.
- [17] Prins E.M., and J. Schmetz (2000). Diurnal active fire detection using a suite of international geostationary satellites. In *Forest Fire Monitoring and Mapping: A Component of Global Observation of Forest Cover*, (F. Ahern, J.-M. Grégoire and C. Justice, eds.), pp.139-148. European Commission Joint Research Centre, EUR19588EN.
- [18] Roberts G., M.J. Wooster, G.L.W. Perry, N. Drake, L-M. Rebelo and F. Dipotso (2005). Retrieval of biomass combustion rates and totals from fire radiative power observations: application to southern Africa using geostationary SEVIRI Imagery. *Journal of Geophysical Research* 110, D21111: doi: 10.1029/2005JD006018.
- [19] Roberts G.J. and M.J. Wooster (2008). Fire detection and fire characterization over Africa using Meteosat SEVIRI. *IEEE Transactions on Geoscience and Remote Sensing*, Vol. 46, No. 4, pp. 1200-1218.
- [20] Roberts G.J., M.J. Wooster, W. Xu, P.H. Freeborn, J.-J. Morcrette, L. Jones, A. Benedetti and J. Kaiser (2015). LSA SAF Meteosat FRP Products: Part 2 – Evaluation and demonstration of use in the Copernicus Atmosphere Monitoring Service (CAMS). *Atmospheric Chemistry and Physics Discussions*, 15, 15909-15976: doi:10.5194/acpd-15-15909-2015.
- [21] Schmetz J., P. Pili, S. Tjemkes, D. Just, J. Kerkmann, S. Rota and A. Ratier (2002). An introduction to Meteosat Second Generation (MSG), *Bulletin of the American Meteorological Society* 83 (7), pp. 977–992 doi:10.1175/1520-0477(2002)083
- [22] Wooster M.J., G. Roberts, P.H. Freeborn, W. Xu, Y. Govaerts, R. Beeby, J. He, A. Lattanzio, and R. Mullen (2015). Meteosat SEVIRI Fire Radiative Power (FRP) products from the Land Surface Analysis Satellite Applications Facility (LSA SAF) – Part 1: Algorithms, product contents and analysis. *Atmospheric Chemistry and Physics Discussions*, 15, 15831–15907: doi:10.5194/acpd-15-15831-2015.